

## **DYNAMICAL BEHAVIOR OF A WIND TURBINE POWER TRAIN CONSIDERING A ROTOR-GEARBOX-GENERATOR COUPLED MODEL**

**Rafael M. Teixeira<sup>1</sup>, Flavia M. Ohara<sup>2</sup>, Matheus D. Milhomens<sup>3</sup>, Aline S. de Paula<sup>4</sup>**  
Universidade de Brasília, Department of Mechanical Engineering 70.910.900 - Brasília-DF, Brazil  
rafaelm.teixeira@hotmail.com  
fla\_mo@hotmail.com  
mdmilhomens@gmail.com  
alinedepaula@unb.br

**Keywords:** Wind turbine, electromechanical dynamics, power train, rotor, gearbox, generator.

**Abstract.** *The world's energy demand is growing with increasing population and development in emerging markets. Electricity generation from fossil fuels, which represent the main source of energy in the world, is responsible for a significant amount of land, water and air pollution due to CO<sub>2</sub> production as well as other greenhouse gases emissions. In this context, the use of renewable energy sources has gained a lot of attention in the last decades, as solar, biomass and wind energies. Considering the high wind energy potential worldwide, wind turbine modeling and analysis has been studied by several authors recently. The goal is to have a better understanding of the system behavior in order to increase the efficiency in the energy conversion and reduce the cost. The electromechanical dynamics of power train-which is composed mainly by the rotor, gearbox and generator - plays an important role on the turbine performance. In the literature, it is usual to focus on the modeling of one of these three elements and consider simplified dynamics to the others. In this paper, a complete model is considered, named rotor-gearbox-generator coupled model, where the three elements are focused on with the goal of obtaining a more realistic representation of wind turbines power train. The gear box considered in this work consists in a two-stage planetary with epicyclicgearing, while a permanent magnet synchronous generator is considered. The dynamical behavior is evaluated for different loads showing system behaviorand energy conversion efficiency.*

## 1 INTRODUCTION

The challenges posed by the need to implement policies that ensure sustainable development are particularly relevant in the field of energy. Increasingly it is faced the need to find in renewable energy a real and feasible way of electricity production when comparable to conventional energy sources, whose are responsible for serious environmental threats.

Wind power is a clean and renewable alternative to the production of electricity, which is aligned with the goals proposed by the Kyoto Protocol, since its use contributes to the reduction of greenhouse gases, especially in countries whose energy matrix is predominantly fossil. Unlike hydroelectric plants, wind farms do not cause expropriation areas and relocation of people. Thus, wind energy is well accepted in social and environmental points of view [6].

A wind turbine is a system composed basically of a rotor, a low-speed input shaft, a gearbox (speed multiplier), a high-speed output shaft and a generator. Figure 1 shows the components of the turbine.

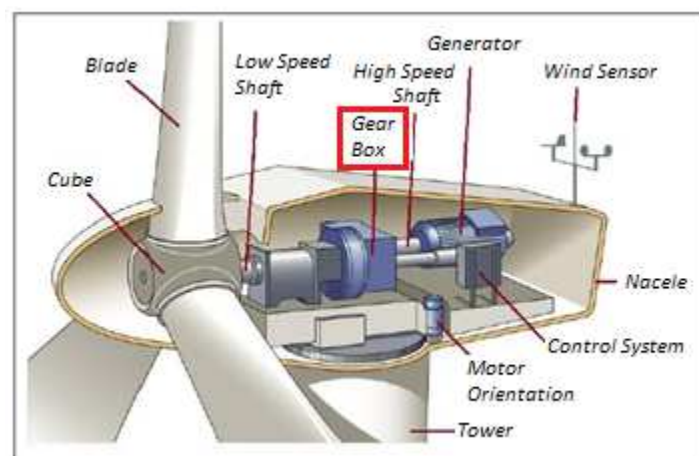


Figure1. Components of a wind turbine.

Wind turbines are devices capable of converting kinetic energy of the wind into electrical energy. Its operation consists in the rotation of rotor blades due to the force of the wind, which is connected to a low speed shaft. This shaft is then coupled to a multiplier box in order to obtain a high speed shaft, which is responsible for driving an electrical generator.

One of the most important components in the wind turbines is the Gear Box, highlighted in Figure 1, which is responsible for increasing the shaft rotation providing appropriate speed to the generator.

Several research papers on wind turbines are currently being published. However, it is usual to focus on the modeling of one of the three principal elements (rotor, gear box, generator) and consider simplified dynamics to the others.

Betz [3], Heir [7], Busawon [4] and Johnson [9] presented studies related to the dynamics of the wind turbine rotor. Still related to the rotor, Manyoge [12] presented a mathematical model to describe the power coefficient behavior, which is used in the present work. Peeters [16][17], Todorov [18], Wei Shi [20], Datong [5], Wang [21] and Helsen [8] studied mathematical models related to the gearbox of wind turbines (the mechanical part of the power train). Regarding the generator, Marques [13], Bernardes [2], Ming Yin [14], Bastos [1] and Lei [11] studied mathematical models related to the generator. Vásques [19] developed mathematical models of permanent magnet synchronous generators for hydrokinetic systems. Given the similarity with wind systems, the model is perfectly feasible to wind turbines and is used in the present work.

From the literature, there is a clear separation between works that considers mechanical and electrical analysis. The goal of this work is to analyze the dynamics of the power train considering a complete electromechanical model, that contemplates the coupled dynamics of rotor, gearbox and generator.

## 2 ROTOR-GEARBOX-GENERATOR MODEL

### 2.1 Rotor

The rotor is the component responsible for transforming the kinetic energy of the wind into rotational mechanical energy. Considering rotor configuration, there are two types of wind turbines: upwind and downwind. In the upwind turbines, the rotor is positioned in front of the tower. Unlike the downwind, where the rotor stays behind the tower.

Rotors with 3 blades are more common because they present a good relation between power ratio, cost and speed of rotation, as well as better aesthetics compared to 2-bladed turbines. This work is based on an upwind rotor with 3 blades.

#### 2.1.1 Power extracted from the wind

The power extracted from the winds depends on several variables such as air density, wind speed, rotor rotation and rotor geometry. The definition of extracted power, given by Busawon [4], is shown un Eq. (1) and represents the mechanical power related to the rotational behavior of the rotor.

$$P_{mec} = \frac{1}{2} \rho \pi r^2 V_0^3 C_p(\lambda, \beta) \quad (1)$$

where  $\rho$  is the air density,  $r$  is the radius of the rotor,  $V_0$  is the wind speed, and  $C_p$  is the power coefficient, which depends on the blade tip velocity ratio  $\lambda$ , the rotor blade geometry and the number of Reynolds of the flow in relation to the diameter of the rotor [18].

There are expressions for  $C_p$  determined numerically, as the one presented by Heier [7], that brings an approximation in terms of  $\lambda$  and  $\beta$ , as follows:

$$C_p(\lambda, \beta) = a_1 \left( \frac{a_2}{\lambda_i} - a_3 \beta - a_4 \beta^{a_5} - a_6 \right) e^{-\frac{a_7}{\lambda_i}} \quad (2)$$

where the term  $\lambda_i$  is given by:

$$\lambda_i = \frac{1}{\frac{1}{\lambda + a_8 \beta} - \frac{a_9}{\beta^{3+1}}} \quad (3)$$

The constants  $a_i$  with  $i = 1, \dots, 9$  can be modified according to the type of turbine to be analyzed for better adjustment.

Once the extracted power is determined by Eq. (1), the mechanical input torque of the turbine is given as presented in Eq.(4).

$$T_{mec} = \frac{P_{mec}}{\omega_{rot}} \quad (4)$$

where  $\omega_{rot}$  is the speed of the output shaft of the rotor.

## 2.2 Gearbox

The multiplier box of the wind turbines is responsible for transmitting the mechanical energy delivered by the rotor shaft to the generator and is necessary for the input speed to be multiplied to suit the speed required for the electric generator. They are usually made up of shafts, drive gears and couplings.

The gearbox model developed in this work, shown in Fig. 2, is a commercial model of the company TGM, with a multiplication system composed of two stages in series of epicyclic trains.

One train is composed of four planets gears and while the other has three. Fig.2 shows a schematic picture of the gearbox, whose symbol  $J_i$  refers to the moment of inertia,  $Z_i$  the number of teeth of the gears,  $m_i$  the masses of the planets gears,  $r_{c,i}$  the radius of the Carrier arms, and  $\varphi_i$  the absolute angular displacement of a fixed coordinate. The index  $i = 1, 2, 3, 4, R_1, 5, 6, 7, R_2, 8$  correspond to the rotor, carrier (2), planet gears, sun gear and ring gear of the first stage, carrier (5), planet gears, sun gear and ring gear of the second stage and the generator, respectively.  $K_1, K_2, K_3$  refers to the stiffness of each shaft.

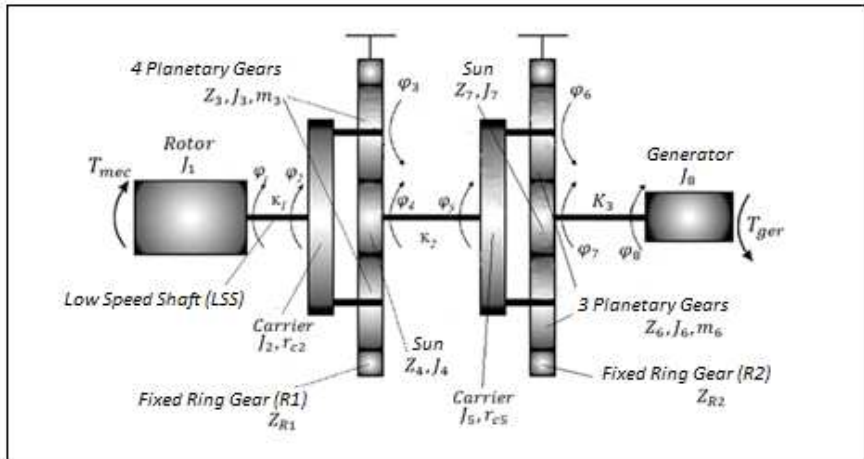


Figure 2. Schematic drawing of the gearbox TGM.

Mathematical modeling is performed by applying the Lagrange equations, and considering totally rigid bodies (except axles) and all rotational only motions (except planetary gears that have tangential translation movements to the sun gears).

Considering the gear ratios  $\gamma$ , using the number of teeth  $Z_r$  and  $Z_o$  of the gears shown in Eq. 5, we have the kinematic relations (Eq. 6), used in the system model [15].

$$\begin{aligned} \gamma_1 &= 1 - (Z_{r1}/Z_3) \gamma_2 = 1 + (Z_{r1}/Z_4) \\ \gamma_3 &= 1 - (Z_{r2}/Z_6) \gamma_4 = 1 + (Z_{r2}/Z_7) \end{aligned} \quad (5)$$

$$\begin{aligned}\dot{\phi}_3 &= \gamma_1 \dot{\phi}_2 \dot{\phi}_4 = \gamma_2 \dot{\phi}_2 \\ \dot{\phi}_6 &= \gamma_3 \dot{\phi}_5 \dot{\phi}_7 = \gamma_4 \dot{\phi}_5\end{aligned}\quad (6)$$

Simplifying the equations of the system, using the relations shown in Eq. 6, we obtain the system of only 4 degrees of freedom.

Eq. (7) shows the four equations of motion for the multiplier set.

$$\begin{aligned}\varphi_1: J_1 \ddot{\phi}_1 + K_1 \varphi_1 - K_1 \varphi_2 &= T_{mec} - \mu_1 \tan(\phi_1 e^6) - C_1 \dot{\phi}_1 + C_1 \dot{\phi}_4 \\ \varphi_2: [J_2 + 4m_3 r_{c2}^2 + 4J_3 \gamma_1^2 + J_4 \gamma_2^2] \ddot{\phi}_2 + [K_1 + \gamma_2^2 K_2] \varphi_2 - K_1 \varphi_1 - \gamma_2 K_2 \varphi_5 &= \\ -\mu_2 \tan(\phi_2 e^6) - C_1 \dot{\phi}_2 - (C_1 + \gamma_2^2 C_2) \dot{\phi}_5 & \\ \varphi_5: [J_5 + 3m_6 r_{c5}^2 + 3J_6 \gamma_3^2 + J_7 \gamma_4^2] \ddot{\phi}_5 + [K_2 + \gamma_4^2 K_3] \varphi_5 - \gamma_2 K_2 \varphi_2 - \gamma_4 K_3 \varphi_8 &= \\ -\mu_3 \tan(\phi_5 e^6) + C_2 (\gamma_2 \dot{\phi}_5) - C_2 + \gamma_4^2 C_3 + C_3 (\gamma_4 \dot{\phi}_8) & \\ \varphi_8: J_8 \ddot{\phi}_8 + K_3 \varphi_8 - \gamma_4 K_3 \varphi_5 &= T_{ger} - \mu_4 \tan(\phi_8 e^6) - C_3 \dot{\phi}_8 + C_3 (\gamma_4 \dot{\phi}_6)\end{aligned}\quad (7)$$

### 2.3 Generator

The generator considered in this work is asynchronous generator of permanent magnets (permanent magnet synchronous generator, PMSG). These generators have high performance and have no slip rings or windings, that are replaced by magnetic elements [2].

Using the mathematical model that defines the dynamics of the generator (synchronous of three-phase protruding poles), the equations of movement of the generator as a function of  $i_d$  e  $i_q$  can be represented by Eq. (8), as detailed by Vásques [19].

$$\begin{aligned}i_d &= (L_L + L_d) \frac{di_d}{dt} = -(R_L + R_S) i_d + (L_L + L_q) \frac{N_p}{2} \omega_{mec} i_q \\ i_q &= (L_L + L_q) \frac{di_q}{dt} = -(R_L + R_S) i_q - (L_L + L_d) \frac{N_p}{2} \dot{\phi}_8 i_d - \frac{N_p}{2} \omega_{mec} \psi_{pm}\end{aligned}\quad (8)$$

where  $i_d$  and  $i_q$  are the currents in the direct axis and the quadrature axis of the generator respectively,  $\omega_{mec}$  is the velocity of the output shaft of the multiplier and  $\psi_{pm}$  is the magnetic coupling flux of the generator.

In a wind turbine, a value of much interest in the project is the power generated. The active power of the generator is given by Eq. 9:

$$P_{ativ} = \frac{3}{2} (V_d i_d + V_q i_q) \quad (9)$$

Another important value is the electrical power that was actually converted from the mechanical power. The electromechanical power of the generator is given by the expression, Eq. (10):

$$P_{ele} = \frac{3}{2} \omega_e (\psi_d i_q - \psi_q i_d) \quad (10)$$

where  $\omega_e$  is the electric angular velocity and  $\psi_d$  and  $\psi_q$  are the direct and quadrature magnetic fluxes respectively.

The power generated is the product of the mechanical speed  $\omega_{mec}$  with the electric torque  $T_{ger}$ .

In this way, the expression for the generator torque shown in Eq.11:

$$T_{ger} = \frac{3N_p}{4} [\psi_{pm} i_q + (L_d - L_q) i_d i_q] \quad (11)$$

### 3 ROTOR-GEARBOX-GENERATOR MODEL COUPLED

Attaching the mechanical (Eqs. 4 e 6) and electrical (Eqs. 8 e 11) parts and considering the state variables  $\{x_1, x_2, x_3, x_4, x_5, x_6, x_7, x_8, x_9, x_{10}\} = \{\varphi_1, \dot{\varphi}_1, \varphi_2, \dot{\varphi}_2, \varphi_5, \dot{\varphi}_5, \varphi_8, \dot{\varphi}_8, i_d, i_q\}$ , the equations of motion can be rewritten as a set of first-order differential equations, Eq. (12). Note that the angular velocity  $\omega_{mec}$  is variable  $\dot{\varphi}_8$  while the speed of the rotor,  $\omega_{rot}$ , is variable  $\dot{\varphi}_1$ .

$$\begin{aligned} \dot{x}_1 &= x_2 \\ \dot{x}_2 &= \frac{-C_1 x_2 + C_1 x_4 - \mu_1 \tan(x_2 e^6) - K_1 x_1 + K_1 x_3 + T_{mec}}{J_1} \\ \dot{x}_3 &= x_4 \\ \dot{x}_4 &= \frac{-C_1 x_2 - (C_1 + \gamma_2^2 C_2) x_4 + \gamma_2 x_6 C_2 - \mu_2 \tan(x_4 e^6) - [K_1 + \gamma_2^2 K_2] x_3 + K_1 x_1 + \gamma_2 K_2 x_5}{J_2 + 4m_3 r_{c2}^2 + 4J_3 \gamma_1^2 + J_4 \gamma_2^2} \\ \dot{x}_5 &= x_6 \\ \dot{x}_6 &= \frac{\gamma_2 x_4 C_2 - (C_2 + \gamma_4^2 C_3) x_6 + \gamma_4 x_8 C_3 - \mu_3 \tan(x_6 e^6) + \gamma_2 K_2 x_3 - [K_2 + \gamma_4^2 K_3] x_5 + \gamma_4 K_3 x_7}{J_5 + 3m_6 r_{c5}^2 + 3J_6 \gamma_3^2 + J_7 \gamma_4^2} \\ \dot{x}_7 &= x_8 \\ \dot{x}_8 &= \frac{C_3 \gamma_4 x_6 - C_3 x_8 - \mu_4 \tan(x_8 e^6) - K_3 x_7 + K_3 \gamma_4 x_5 - T_{ger}}{J_8} \\ \dot{x}_9 &= \frac{-(R_L + R_S) x_9 + (L_L + L_q) \frac{N_p}{2} x_8 x_{10}}{(L_L + L_d)} \\ \dot{x}_{10} &= \frac{-(R_L + R_S) x_{10} - (L_L + L_d) \frac{N_p}{2} x_8 x_9 - \frac{N_p}{2} x_8 \psi_{pm}}{(L_L + L_q)} \end{aligned} \quad (12)$$

The efficiency of the system is also a very important parameter of analysis in the design of a wind turbine. It indicates how much electrical energy can be obtained given an input power. Efficiency is obtained by calculating the ratio of the active power  $P_{ativ}$ , given by Eq. 9, and the mechanical input power,  $P_{mec}$ , as shown in Eq. 13.

$$\eta = \frac{P_{ativ}}{P_{mec}} \quad (13)$$

#### 4 DYNAMIC ANALYSIS OF THE COMPLETE SYSTEM

Analysis is carried out by numerical integration of Eq. (12) using Runge-Kutta of 4th order. Gearbox parameters are provided by TGM and presented in Table 1. Generator parameters are the same used by Tucunaré project [19], as presented in Table 2.

Element	Mass (kg)	Total Inertia (kg.m <sup>2</sup> )	Diameter (mm)	Stiffness (N/m)	Viscous Damping (N/m)
Input axis 1	--	--	--	1.468210 <sup>8</sup>	7.3411x10 <sup>4</sup>
Carrier 2	--	J2=160.9612	676	--	--
Gears Planets 3	20.64	J3=8.7649	--	--	--
Solar gear 4	--	J4=2.2026	--	--	--
Axis 2	--	--	--	0.4203x10 <sup>8</sup>	2.1015x10 <sup>4</sup>
Carrier 5	--	J5=53.0721	588	--	--
Gears Planets 6	11.0867	J6=3.2232	--	--	--
Solar gear 7	--	J7=0.1765	--	--	--
Axis 3	--	--	--	0.0483x10 <sup>8</sup>	0.2417x10 <sup>4</sup>
Generator	--	J8=22.2548	--	--	--

Table 1.TGM gearbox Components information.

Gearbox efficiency $\eta$	Gear ratio	Inductance $L_d$	Resistance $R_s$	Magnetic Flux $\psi_{pm}$	Number of pole pairs
1	10	0,00899995 H	0,0218463 ohm	4,759 Wb	12

Table 2.Input data for the generator [19].

Initially the frequency response is evaluated by the Fast Fourier Transform (FFT) considering the free response of the system. Four different cases are simulated, two considering the mechanical part alone (one with high and other with low damping) and two for the complete model described previously (one with high and other with low damping). The idea of considering at first only the mechanical part is analyze the influence of coupling the electrical part.

For each case, 4 simulations of the free system with respect to the time are performed. In each simulation one of the initial displacements (related to  $J_1, J_2, J_5, J_8$ ) has a nonzero value

equal to 1 radian. The frequency response is calculated to each one of the 4 free responses and the results consists in the sum of all FFTs.

Considering only the mechanical part alone, Figure 3 presents the frequency response to high (A) and low (B) damping. Low damping is considered as 1% of the high damping. From Figure (B) we observe 3 peaks related to natural frequencies, as expected (the zero frequency related to rigid body motion was not activated). When the damping is higher, second and third peaks become together and smaller in amplitude and only one peak is pronounced.

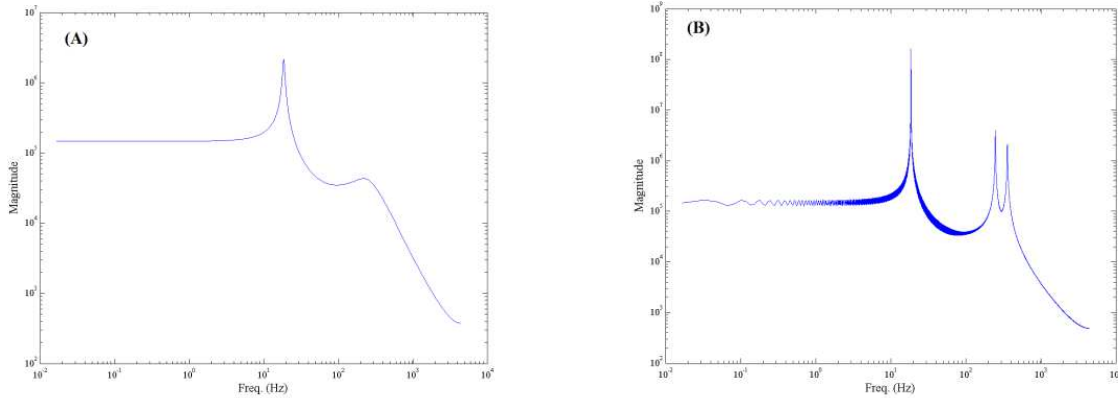


Figure 3. FFT of mechanical alone: (A) High damping; (B) low damping.

Figure 4 shows frequency response for the complete model considering the same damping coefficients used in the results obtained in Figure 3. For the coupled model with smaller damping coefficient, one can observe the presence of some small peaks between the natural frequencies as highlighted in Figure 4B. Note that natural frequency refers to the model that considers only the mechanical part alone. The presence of these small peaks is due to the electric coupling of the generator, that presents nonlinearity.

The results presented in Figures 3 and 4 are one preliminary. Note that system response was considered free, thus, the generator is not really operating. By considering the frequency response when the system is operational, we guess that the influence on the frequency response will be accentuated.

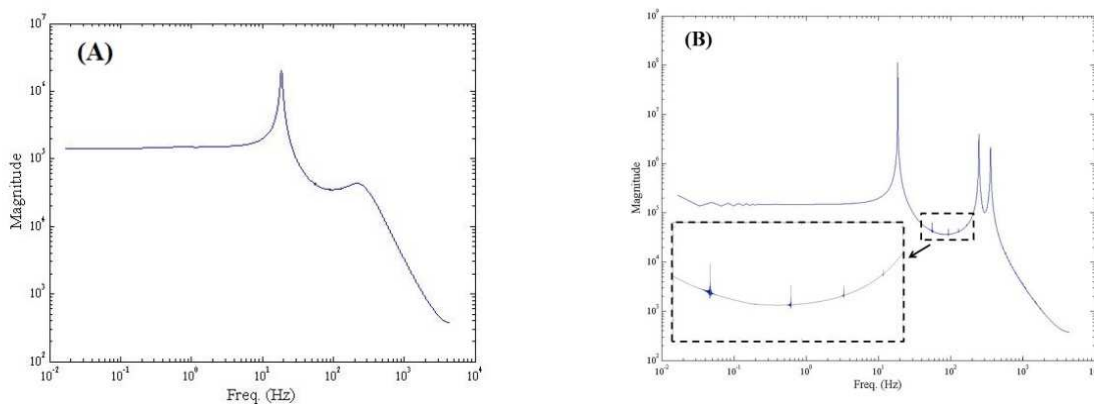


Figure 4. FFT of complete system: (A) high damping; (B) low damping .

At this point, the dynamic behavior of the complete system is of concern. It is considered a wind speed input as shown in Figure 4. In addition, zero initial conditions are considered for



all state variables except for the rotor angular velocity,  $\phi_1$ , equal to 2,35m/s, corresponding to the velocity that generates the maximum  $C_p$  for the angle  $\beta = 5^\circ$  and a wind speed of 15m/s. Figures 6 and 7 show the angular displacements and velocities of the transmission system components for the wind profile considered in Figure 5. Figure 8 shows mechanical and electrical torques presented by the rotor and the generator, respectively, while Figure 9 shows mechanical, active and electromechanical power. Figures 10 and 11 show the efficiency of the transmission system and the power coefficient,  $C_p$ . Finally, Figures 12 and 13 show the currents and voltages in the quadrature axes  $q$  and direct axis  $d$ , respectively, of the generator.

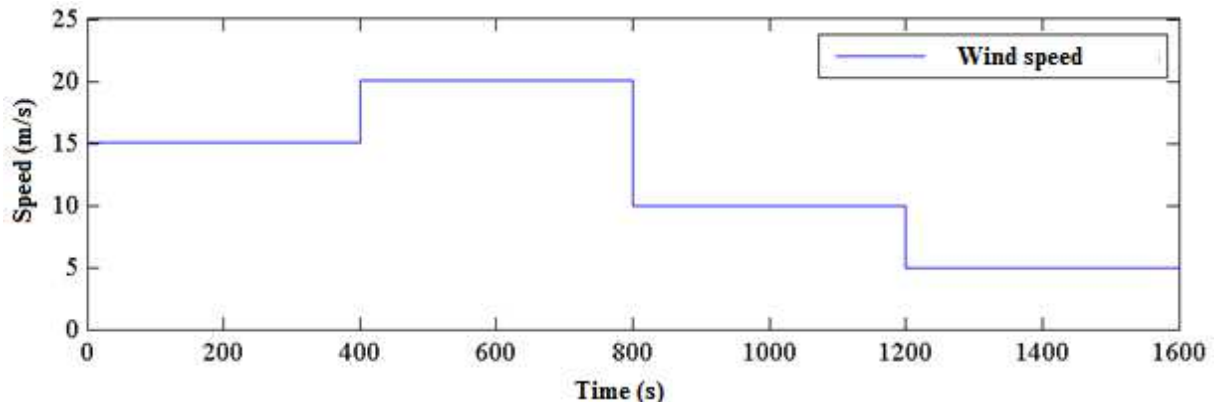


Figure 5. Wind speed input.

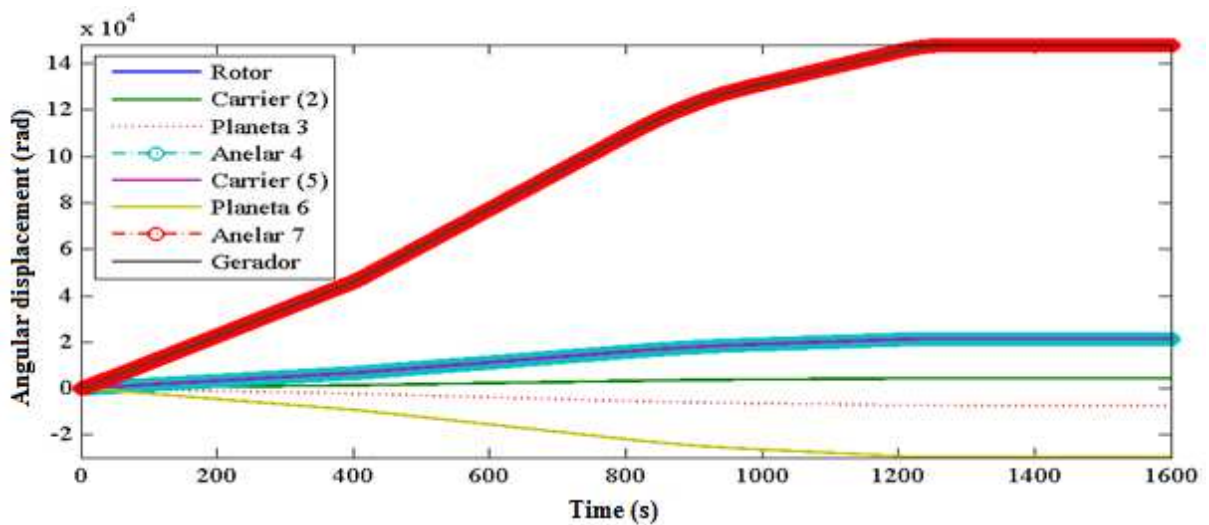


Figure6. Angular displacement of transmission system components.

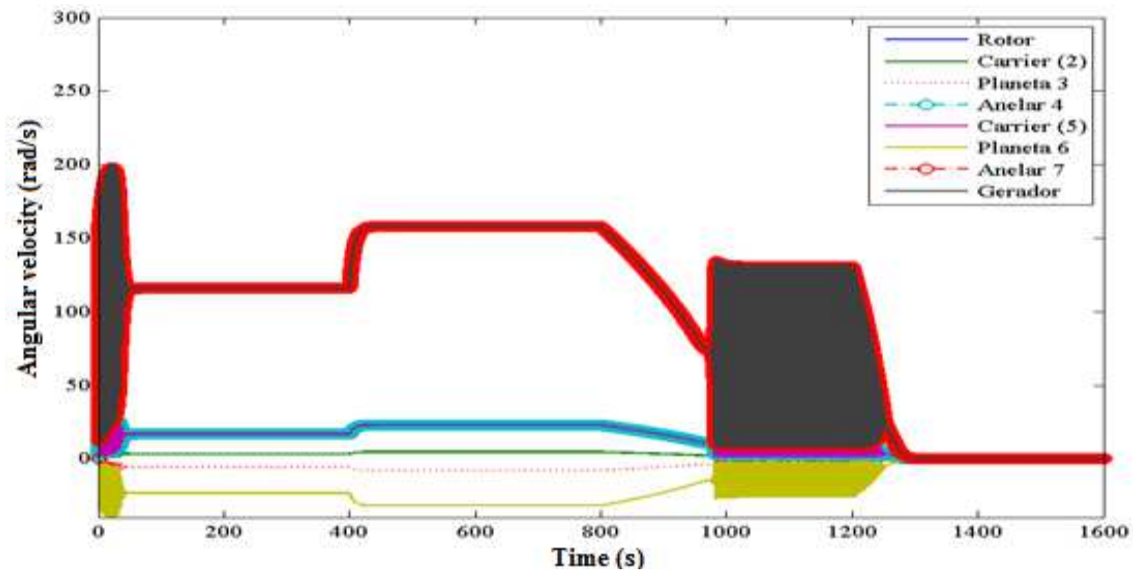


Figure7. Angular velocity of the transmission system components.

It is observed that for wind velocities of 15 to 20m/s, the turbine presents a satisfactory operation after a transient period, as shown in Figure 7. When the speed decreases to 10m/s, the turbine does not stabilize and the angular speeds of the casing components oscillate, resulting in undesired behavior. When the wind speed decreases further, now to 5m/s, the inlet torque becomes insufficient to keep the turbine running.

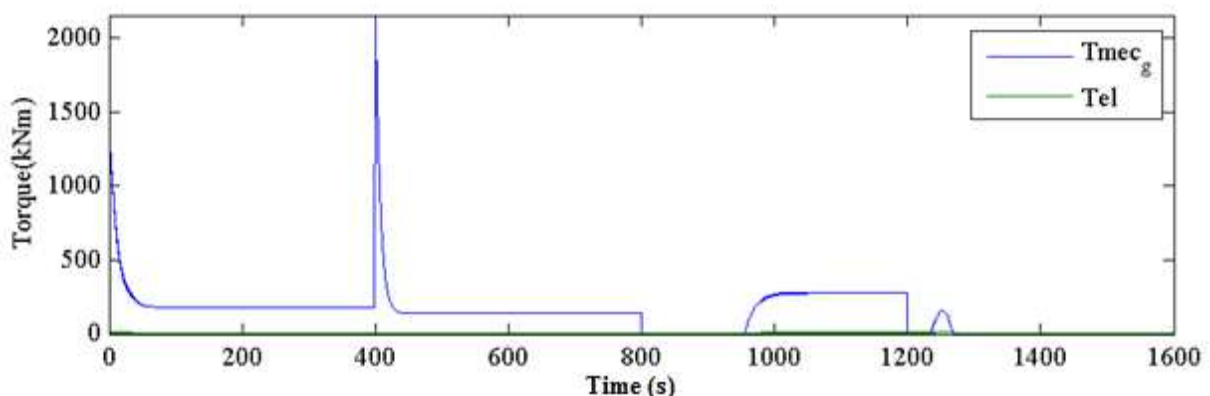


Figure 8. Mechanical and electrical torques of the complete model.

We observed in Fig. 9 that between 800 and 1000 seconds, where the wind speed is 10m/s, the active power is greater than the mechanical input power. This results in an efficiency greater than 1, indicating a physical incoherence.

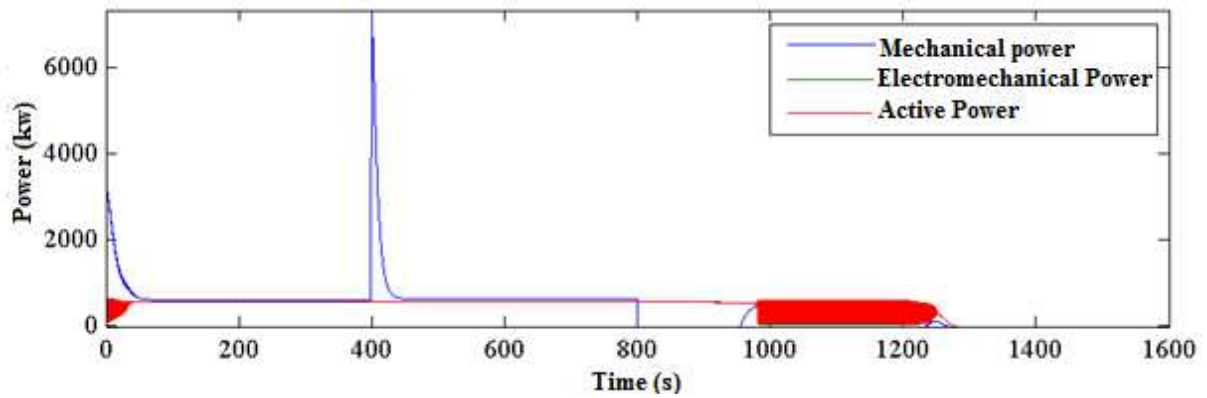


Figure 9. Mechanical, electrical and active powers of the complete model.

It is observed from Fig. 10 that the efficiency of the turbine is higher in the case of wind velocity equal to 15m/s than when it is 20m/s, showing that not always the higher wind speed results in a higher power coefficient.

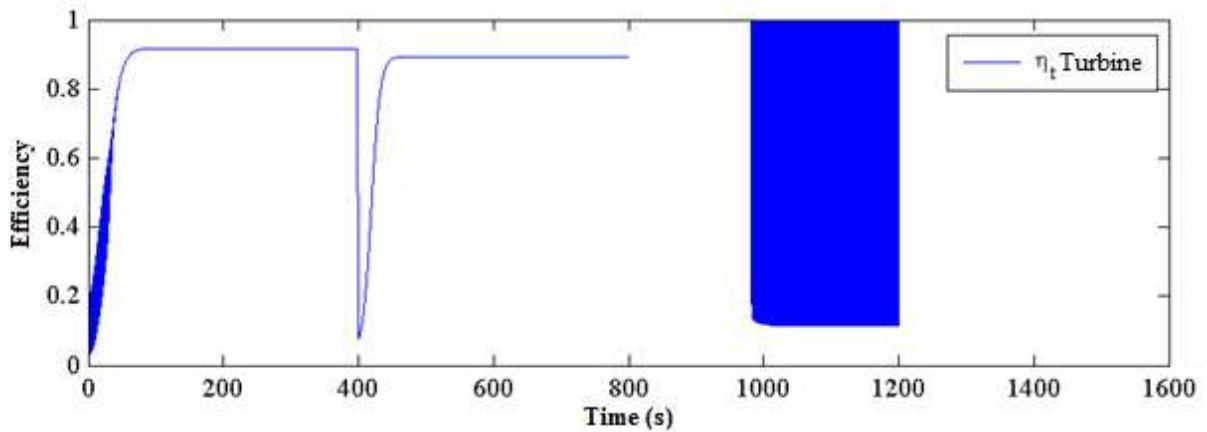


Figure10. Efficiency of the transmission system.

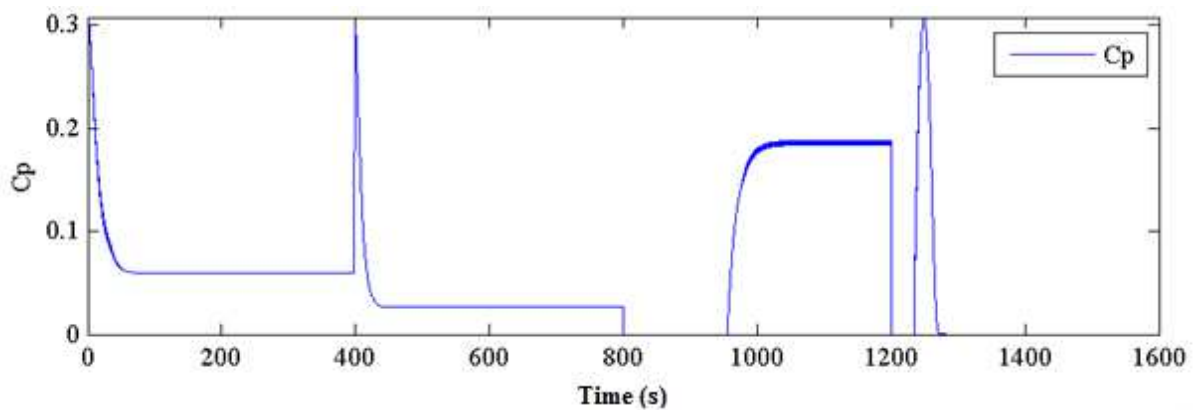


Figure11. Power Coefficient  $C_p$ .

In Fig.11 we observe that  $C_p$  stabilizes in very low values, less than 0.3. It is possible to improve the performance of the system by applying appropriate control to obtain an ideal blade tip speed,  $\lambda$ .

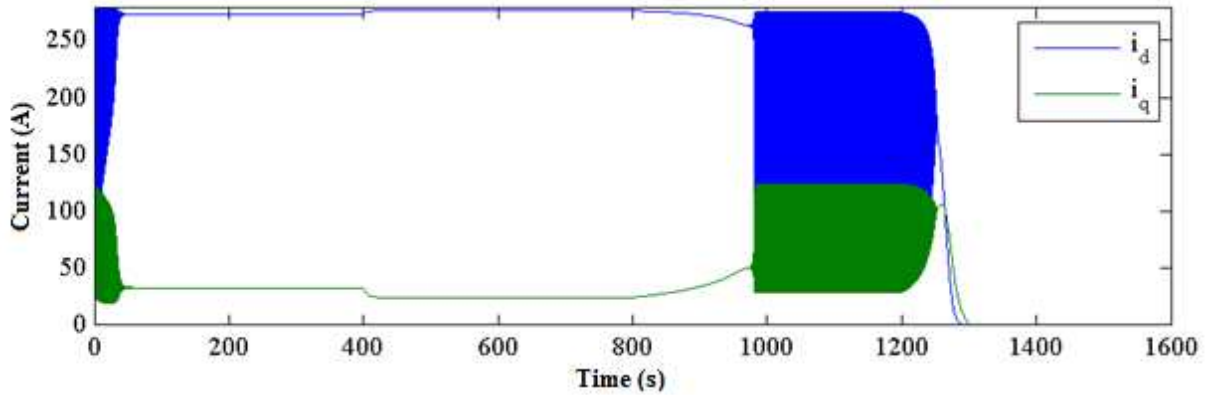


Figure12. Currents  $i_d$  e  $i_q$  for the complete model

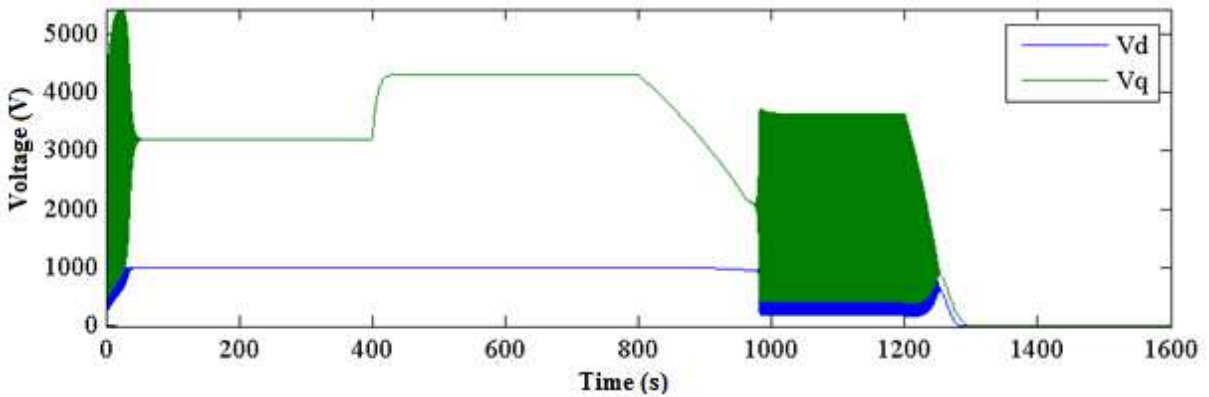


Figure13. Voltages  $v_d$  e  $v_q$  for the complete model

From Figs. 12 and 13, we observe that the currents and voltages remain stable for the first two wind speed variations. Near 1000 seconds of analysis, it is observed that the system destabilizes until it stops when the wind speed reaches 5m/s.

## 5 CONCLUSION

This paper presents a mathematical model for the electromechanical transmission system of a wind turbine, including three main components: rotor, multiplier gearbox and generator. From the analysis in the frequency domain, we observe that when the electrical part is coupled to the mechanical, small peaks appears between the natural frequencies (being natural frequency related to the linear model that considers only the mechanical part). The nonlinearity that comes with the electrical coupling may be responsible for these peaks. The dynamical analysis in time allow a detailed analysis of each component of the system. The development of the complete model allows a more realistic dynamic analysis

## REFERENCES

- [1] Bastos A.F., Cota E.F., Silva S.R., Pereira H.A., Use a newton's method for rotor resistance control of wind turbine generators. In: International conference on renewable energies and power quality – ICREPQ. EA4EPQ; 2012.

- [2] Bernardes T.A. Análise e Controle de Gerador Síncrono a Imã Permanente Aplicado a Sistema de Conversão de Energia Eólica. Dissertação (Mestrado) - Universidade Federal de Santa Catarina, Santa Maria, 2009.
- [3] Betz. A., 1919, Wind-Energie und ihre Ausnutzung durch Windmühlen.
- [4] Busawon, K., Dodson, L., Jovanovic, M., 2005, Estimation of the power coefficient in a wind conversion system, Decision and Control, IEEE Conference on , pp.3450-3455.
- [5] Datong Q., Jianhong W., Qingwei z., "A study on the dynamic behavior of drive train in horizontal wind turbine by a flexible multibody model (Submitted).
- [6] Felippes R.A., Análise e Desenvolvimento de Aerogeradores com Pás Compósitas, Dissertação de Mestrado em Ciências Mecânicas, Departamento de Engenharia Mecânica, Universidade de Brasília, Brasília, 2012.
- [7] Heier, S., 2006, Grid Integration of Wind Energy Conversion Systems. 2ª Ed., John Wiley & Sons, London, Inglaterra.
- [8] Helsen J., Vanhollebeke F., Vandepitte D., Desmet W., "Multibody modelling of varying complexity for modal behaviour analysis of wind turbine gearboxes. Volume 36, Issue 11, November 2011, Pages 3098–3113
- [9] K. E. Johnson, Adaptive Torque Control of Variable Speed Wind Turbines, NREL/TP-500-36265, August 2004.
- [10] Lees, A.W., Friswell, M.I. & Litak, G. (2011), "Torsional Vibration of Machines with Gear Errors", Journal of Physics: Conference Series, v.305 (012020).
- [11] Lei Y., Mullane A., Lightbody G., Yacamini R., Modeling of the wind turbine with a doubly fed induction generator for grid integration studies. IEEE Transactions on Energy Conversion, vol. 21, no. 1, March 2006.
- [12] Manyonge, A., Ochieng, R. M., Onyango, F. N., Shichikha, J. M., 2012. Mathematical Modelling of Wind Turbine in a Wind Energy Conversion System: Power Coefficient Analysis. Applied Mathematical Sciences, v. 6, n. 4527 - 4536.
- [13] Marques, J., 2004, Turbinas Eólicas: Modelo, Análise e Controle do Gerador de Indução com Dupla Alimentação, Universidade Federal de Santa Maria, RS.
- [14] Ming Yin, Li. G., Zhou, Zhao, C., Modeling of the Wind Turbine With a Permanent Magnet Synchronous Generator for Integration, 1-4244-1298-6/07/2007 IEEE.
- [15] Shigley, J. E., Mischke, C. R., Budynas, R.G., 2005, Projeto de Engenharia Mecânica, 7ª Ed., Bookman, São Paulo, SP.
- [16] Peeters R. H.; Vandepitte, D.; Sas, P. Analysis of Internal Drive Train Dynamics in a Wind Turbine. Wiley Interscience, Leuven, p. 1-21, Set. 2005.
- [17] Peeters, J., 2006, Simulation of Dynamic Drive Train Loads in a Wind Turbine, Universidade Católica de Leuven – Bélgica.
- [18] Todorov, M., Dobrev, I., Massouh, F, 2009, Analysis of Torsional Oscillation of Drive Train in Horizontal-Axis Wind Turbine, Electromotion-2009, EPE Chapter Electric Drives, Lille, France, 7 p.
- [19] Vásques, F.A.M., Oliveira, T. F., Brasil, A. C. P., "On the electromechanical behavior of hydrokinetic turbines" Energy Conversion and Management 115 (2016) 60–70
- [20] Wei Shi, Kim C.W., Park H.C., Dynamic Modeling and Analysis of a Wind Turbine Drivetrain Using the Torsional Dynamic Model, International Journal of Precision engineering and manufacturing, Vol. 14, no. 1, pp. 153-159 January 2013.
- [21] Wang J., Qin D., Ding Y., Dynamic behavior of wind turbine by a mixed flexible-rigid multi-body model. Journal of System Design and Dynamics, Vol3, Nº3, 2009.